Journal of Applied Spectroscopy, Vol. 76, No. 3, 2009

X-RAY PHOTOELECTRON SPECTROSCOPY STUDY OF THE ELECTRONIC STRUCTURE OF $La_{1-x}Ca_xMnO_{3+\delta}$ SOLID SOLUTIONS

S. H. Estemirova,[a*] A. V. Fetisov,[a] and V. B. Fetisov[b]

UDC 543.428.3

The electronic structure of $La_{1-x}Ga_xMnO_{3+\delta}$ solid solutions is studied by X-ray photoelectron spectroscopy (XPS). The valence state of the manganese is estimated by various methods: by analyzing the difference in the binding energies of the $Mn2p_{3/2}$ and O1s electronic levels, analyzing exchange splitting in the spectrum of Mn3s, and from the dependence of the binding energy of the XPS spectrum of $Mn2p_{3/2}$ on the calcium concentration. The state of oxidation of the manganese in the compositions containing calcium lies between Mn^{3+} and Mn^{4+}. The efficacies of these methods are compared. A correlation is found between the type of crystalline structure of $La_{1-x}Ga_xMnO_{3+\delta}$ ($0 \le x < 1$) and the binding energy of the $Mn2p_{3/2}$ peak.

Keywords: *X-ray photoelectron spectroscopy, $La_{1-x}Ga_xMnO_{3+\delta}$, oxygen nonstoichiometry, polymorphic structure, solid solution.*

Introduction. Questions regarding the valence state of transition metals in complex multicomponent systems are a constant subject of discussion, since this topic is connected with the most important problems of modern physical chemistry, such as high temperature superconductivity of cuprates, giant magnetic resistance of manganites, etc. There are a number of distinctive features of defect formation during heterovalent displacements in these complex oxides that are not yet fully understood and require profound, thorough study.

When perovskite-like lanthanum manganite $LaMnO_3$ is doped, the induced charge disorder is compensated by a change in the valence of the Mn atoms, which leads to the giant magnetoresistance effect. Thus, replacement of La by calcium leads to the appearance of quadrivalent manganese in the crystalline lattice of lanthanum manganite: $La^{3+}_{1-x}Ca^{2+}_xMn^{3+}_{1-x}Mn^{4+}_xO_3$. A similar result follows from an excess amount of oxygen in the oxide (self doping). It is believed by some that, with these two types of doping, a "charge disproportionation" reaction takes place, so that within the structure, a more stable configuration than Mn^{3+}–Mn^{4+} develops, Mn^{2+}–Mn^{4+} [1].

Another important question in research on defect formation in the manganites is the degree of localization of the introduced charge on manganese ions. Thus, a redistribution of the electron density between the copper and oxygen in the cuprate high temperature superconductor $YBa_2Cu_3O_{6+\delta}$ as δ is varied regulates many of its physical and chemical properties, including the Curie temperature T_c [2].

In these and many other cases, when it is necessary to obtain direct information on the charge state (based on which the valence, degree of localization of the valence electrons, etc., are evaluated) of some element in a substance, use is made of x-ray photoelectron spectroscopy (XPS). Then the object of study is the so-called "chemical shift" in the lines of the XPS spectrum corresponding to the given element. Because of an effect owing to the crystallographic surroundings (through the Madelung energy of the crystal) on the chemical shift for the transition metals that masks the corresponding effect owing to the valance shell, interpreting the XPS data is more difficult. Thus, attempts have been made to determine the valance state of manganese by means of a deeper analysis of the XPS spectra (studying the distances between lines and other features) [3–6]. In many particular cases, these attempts have been extremely successful, which means that the further development of this approach offers some promise.

*To whom correspondence should be addressed.

[a]Institute of Metallurgy, Urals Branch of the Russian Academy of Sciences, 101 ul. Amundsena, Ekaterinburg, 620016, Russia; e-mail: esveta100@mail.ru; [b]Urals State University of Economics, Ekaterinburg, Russia. Translated from Zhurnal Prikladnoi Spektroskopii, Vol. 76, No. 3, pp. 419–427, May–June, 2009. Original article submitted August 12, 2008.

 0021-9037/09/7603-0394

In this paper we present some results of an XPS study of the electronic structure of the solid solution $La_{1-x}Ca_xMnO_{3+\delta}$. Based on a correlation between the compositional parameters (x, δ) of the structure and the characteristics of the electron spectra that were obtained, some information was obtained on the regions of existence for different valence forms of manganese in $La_{1-x}Ca_xMnO_{3+\delta}$. The effectiveness of these correlations for determining the valence state of manganese ions is discussed.

Experiment. Samples of $La_{1-x}Ca_xMnO_{3+\delta}$ (x = 0.00, 0.06, 0.10, 0.20, 0.40, 0.50, 1.00) were synthesized using ceramics technology from the corresponding oxides, as described elsewhere [7]. In order to obtain samples with a specified oxygen content, the compositions were annealed under certain conditions (temperature, atmosphere) which we established in the preliminary stages of this research: samples with a stoichiometric oxygen content were obtained by final annealing in air at a temperature of 1573 K; samples with excess oxygen, by annealing in an O_2 atmosphere at 1173 K. Annealing was terminated by quenching the ceramic material on a massive copper plate. Final annealing of the composition $LaMnO_{2.89}$ with an oxygen deficiency was carried out at 1273 K in an argon atmosphere with a partial pressure of oxygen of $\sim 10^{-13}$ Pa in a special enclosed apparatus with electrochemical techniques for maintaining low P_{O_2}. The sample was quenched by removing the operating part of the system from the heating zone and then cooling it with water. Formation of a single phase produce was checked by x-ray phase analysis using a DRON-2 x-ray diffractometer (CuK_α emission, Ni filter). The parameters of a unit cell were determined from 18–20 reflections. The absolute oxygen contents were determined by reducing the samples in a hydrogen atmosphere until the stable oxides were attained.

The XPS studies were conducted on a spectrometric system based on a Multiprob Compact vacuum system equipped with an EA-125 (Omicron, Germany) energy analyzer. The excitation radiation source was an x-ray gun with an aluminum anode. The energy scale of the energy analyzer was calibrated using standard samples: Au, Ag, and Cu. In order to take the "charging" of the samples during electron emission into account, the positions of the lines in the XPS spectrum were corrected with respect to the position of the C1s line of carbon belonging to the $(CH)_n$ groups, assuming its binding energy to be E_b = 285.0 eV.

Prior to the XPS studies, the surfaces of the samples were cleaned mechanically with a scraper in the mounting chamber until the "carbonate" C1s peak (~289 eV) vanished and the shape of the oxygen O1s peak no longer varied. It should be noted that a high energy shoulder in the spectrum of O1s (see the inset in Fig. 1) has been observed in a number of papers (e.g., [3]). Its presence is usually attributed to the presence on the sample surface of either hydroxyl groups or weakly bound oxygen [3, 6]. In some papers, this shoulder vanishes completely after prolonged mechanical cleaning of the surface [8]. The XPS spectra were analyzed using the program XPS PEAK 4.1 [9]. After background subtraction by the Shirley method, the experimental curve was deconvolved with optimal minimizing of the number of peaks used to describe it.

Discussion of Results. The x-ray phase and x-ray structural analyses show that all the synthesized samples are of a single phase and have a perovskite-like structure in the form of three polymorphic modifications, whose type depends on the method and degree of doping of the $La_{1-x}Ca_xMnO_{3+\delta}$ (Table 1). As an example, Fig. 1 shows the complete XPS spectrum of one of the samples, with the spectral features of interest to our study indicated thereon.

XPS spectra of 3d-lanthanum and 2p-calcium. The $3d_{1/2}$ line of lanthanum (Fig. 2) has the complex structure typical of this element, with s–d spin orbital splitting and a separation of ~4 eV between the split peaks. The binding energy of this line has a tendency to decrease with increasing composition parameter x. For the samples with x = 0.0, 0.1, and 0.2 with an excess oxygen content, the spectrum of La3d is shifted to lower E_b relative to the oxides with a stoichiometric composition (Table 2). Note that a shift in the La3d spectrum into the lower energy region has also been observed [3] as the amount of strontium in stoichiometric $La_{1-x}Sr_xMnO_3$ is increased. In these compounds, lanthanum manifests a stable oxidation state of +3, so the chemical shift with increasing x observed for it (see Table 2) can be attributed to changes taking place in its crystallographic surroundings. Thus, it has been shown [10] that, as the coordination number for the La atoms increases, the La3d doublet is shifted toward lower E_b. In addition, it has been found [11] that after chemical etching and ion cleaning of $La_{0.8}Ca_{0.2}MnO_3$ (so that an anion deficient surface is formed), as the concentration of oxygen vacancies is increased the split $3d_{5/2}$ peak is shifted toward higher E_b, while the split parameter increases.

The binding energy of the Ca2p electronic level in $La_{0.8}Ca_{0.2}MnO_3$ falls off noticeably as the calcium concentration is raised (Table 2). Here the difference in E_b for the opposite limits of the solid solution for the compounds

TABLE 1. Unit Cell Parameters of $La_{1-x}Ca_xMnO_{3+\delta}$

Composition	Spatial group	a, Å	b, Å	c, Å	β, deg.	Unit cell volume per unit structural element, V/Z, Å^3
$LaMnO_{2.89}$	$P112_1/c$ (M)	5.7248(41)	7.7082(65)	5.5385(69)	90.006	61.099
$LaMnO_3$	$P112_1/c$ (M)	5.5951(23)	7.7348(42)	5.5340(32)	90.084 (27)	59.865
$LaMnO_{3.15}$	$R\bar{3}c$ (R)	5.4809(55)	–	–	60.592 (94)	58.989
$La_{0.90}Ca_{0.10}MnO_3$	$Pnma$ (O)	5.5378(30)	7.785(41)	5.5411(55)	–	59.721
$La_{0.90}Ca_{0.10}MnO_{3.09}$	$R\bar{3}c$ (R)	5.4726(55)	–	–	60.571 (93)	58.694
$La_{0.80}Ca_{0.20}MnO_3$	$Pnma$ (O)	5.4962(36)	7.7740(42)	5.4987(23)	–	58.736
$La_{0.80}Ca_{0.20}MnO_{3.02}$	$Pnma$ (O)	5.4822(3)	7.7540(4)	5.5050(3)	–	58.503
$La_{0.70}Ca_{0.30}MnO_3$	$Pnma$ (O)	5.4734(6)	7.7366(7)	5.4849(4)	–	58.064
$La_{0.65}Ca_{0.35}MnO_3$	$Pnma$ (O)	5.4623(10)	7.7164(27)	5.4741(17)	–	57.682
$La_{0.50}Ca_{0.50}MnO_3$	$Pm3m$ (C)	3.8282(4)	–	–	–	56.103
$CaMnO_3$	$Pm3m$ (C)	3.7325(5)	–	–	–	51.999

Notes. M indicates monoclinic crystalline system, O orthorhombic, R rhombohedral, and C cubic.

$LaMnO_3$ and $CaMnO_3$ is ~1 eV. The valence of calcium in these compounds is also stable (+2), so the observed shift of Ca2p (as that of La3d) can be attributed to changes taking place in the crystallographic surroundings of Ca.

XPS spectra of manganese and oxygen. It is known that the physical and chemical properties of doped manganites are mainly determined by the state of the manganese ions. As mentioned above, there are two alternative models which describe the electronic configurations of the Mn ions in different ways. One of these is the "charge disproportionation" model, which, on the basis of data regarding the instability of $Mn^{3+}\cdots Mn^{3+}$ complexes, assumes the existence in $La_{1-x}Me_xMnO_{3+\delta}$ (Me is a bivalent metal) of more stable $Mn^{2+}\cdots Mn^{4+}$ pairs. This assumption is confirmed by the observed [1, 12] characteristic behavior of the thermal emf and electrical resistance as functions of temperature. According to the other model, the Mn^{2+} configuration does not exist, but coexistence of the Mn^{3+} and Mn^{4+} ions is more probable for this system [5].

In reality, determining the valence state of manganese in $La_{1-x}Me_xMnO_3$ (including by XPS) is far from a trivial task. According to handbook data [13], the values of E_b for the Mn2$p_{3/2}$ electronic level in the simple oxides Mn(II), Mn(III) and Mn(IV) are 641.0, 641.5, and 642.6 eV, respectively, which means that these states can be distinguished quite reliably. However, in the crystalline structures of $LaMnO_3$ and $CaMnO_3$, as well as the intermediate compositions, the positions of these peaks are so close that it is not possible to isolate the different states in the spectrum of Mn2p.

As an instrument for analyzing the valence state of manganese in $La_{1-x}Ca_xMnO_3$ it has been proposed [6] that the difference in the binding energies of Mn2$p_{3/2}$ and O1s be used. In this case the opposite shifts of the oxygen and manganese peaks (which depend on x or δ) are summed, yielding a larger effect. When this method is used, there is also a significant reduction in the error in the determination of the unknown quantity, since the effect owing to the "charging" of the sample vanishes. The difference in E_b for the Mn2$p_{3/2}$, O1s pair may reach 0.6–0.7 eV as the oxidation state of the manganese increases [6]. The dependence of the difference in the binding energies of Mn2$p_{3/2}$ and O1s on the parameter x that we obtained for $La_{1-x}Ca_xMnO_3$ compositions which are stoichiometric in oxygen (Fig. 3a) is linear and is in good agreement with the results obtained by others. The linear dependence is an indication that the spectrum responds proportionally to a change in the state of the manganese from Mn^{3+} in $LaMnO_3$ to Mn^{4+} in $CaMnO_3$.

Another way of estimating the valence of Mn is the analysis of spectrometric data on exchange splitting (ΔS) of the Mn3s electronic level, which leads in most cases to reliable results that are confirmed by the other methods. The high reliability of this method is based on the fact that ΔS depends strictly on the number of electrons in the 3d

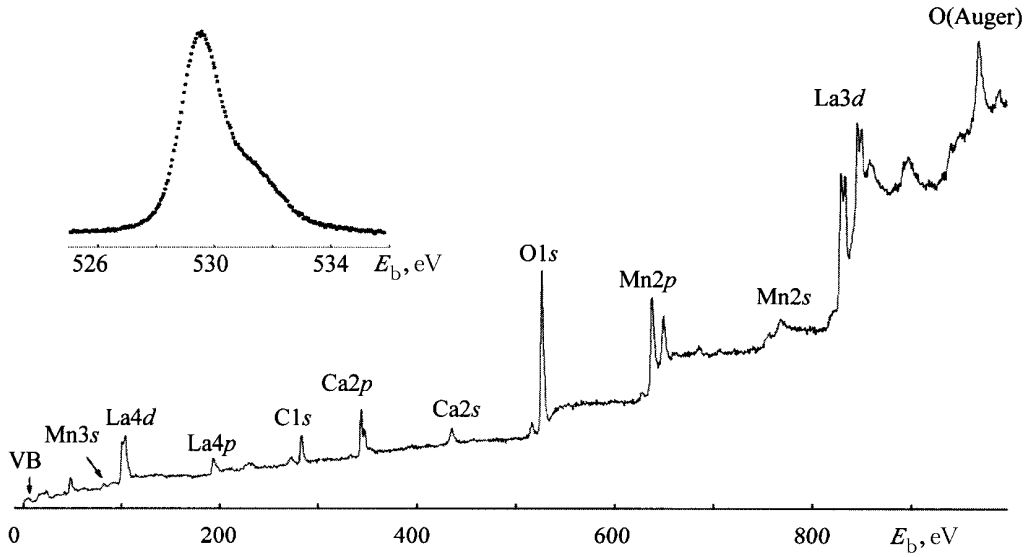

Fig. 1. Survey XPS spectrum of $La_{0.5}Ca_{0.5}MnO_3$; the inset shows the 1*s* spectrum of oxygen for the same sample (after background subtraction).

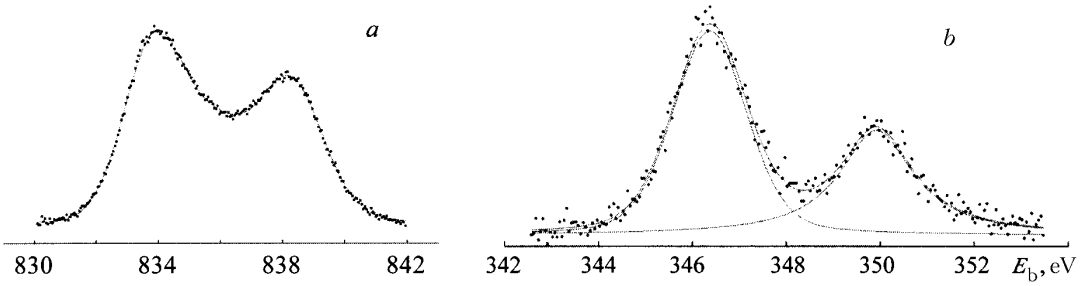

Fig. 2. XPS spectra of the core levels of La3$d_{5/2}$ (a) and Ca2p (b) for $La_{0.3}Ca_{0.3}MnO_3$.

TABLE 2. Binding Energies of the X-Ray Photoelectron Peaks of La3$d_{5/2}$ and Ca2$p_{3/2}$ in $La_{1-x}Ca_xMnO_{3+\delta}$ Solid Solution

Composition	E_b(La3$d_{5/2}$), eV	E_b(Ca2$p_{3/2}$), eV
$LaMnO_3$	833.96	–
$LaMnO_{3.15}$	833.89	–
$La_{0.94}Ca_{0.06}MnO_3$	834.00	346.75
$La_{0.90}Ca_{0.10}MnO_3$	833.91	346.59
$La_{0.90}Ca_{0.10}MnO_{3.09}$	833.79	346.64
$La_{0.80}Ca_{0.20}MnO_3$	833.85	346.39
$La_{0.80}Ca_{0.20}MnO_{3.02}$	833.85	346.50
$La_{0.70}Ca_{0.30}MnO_3$	833.85	346.37
$La_{0.50}Ca_{0.50}MnO_3$	833.58	346.07
$CaMnO_3$	–	346.57

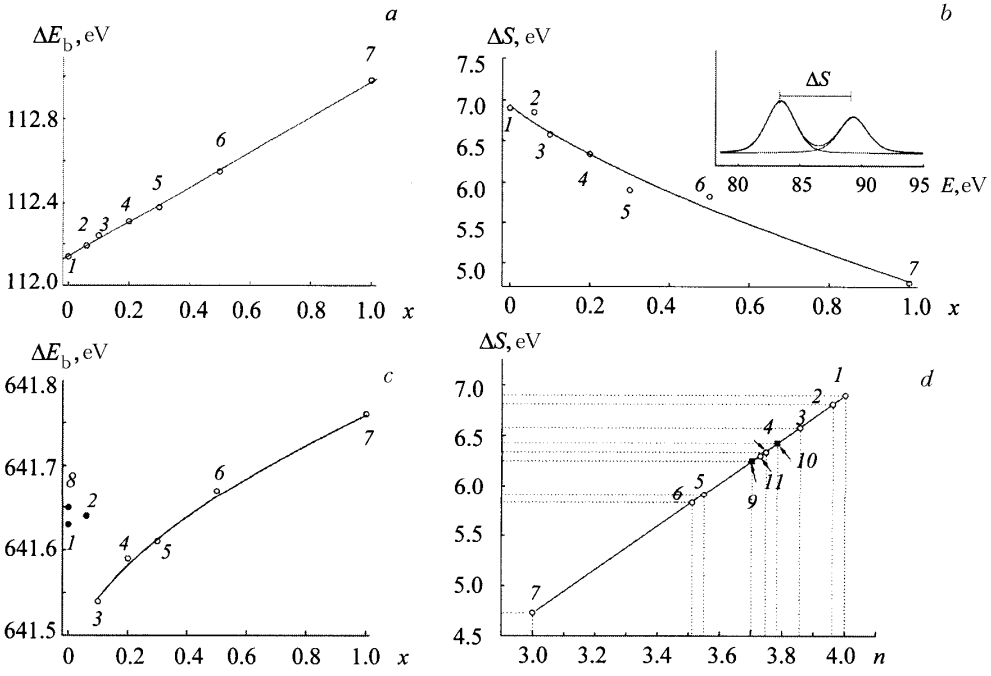

Fig. 3. Methods for estimating the valence state of manganese in the solid solution $La_{1-x}Ca_xMnO_{3\pm\delta}$: (a) by analyzing the difference in the binding energies (ΔE_b) of the Mn2$p_{3/2}$ and O1s electronic levels; (b) by analyzing the exchange splitting of the spectrum of Mn3s (ΔS); the inset shows the XPS spectrum of Mn3s for sample No. 6; (c) from the dependence of the binding energy of the XPS spectrum of Mn2$p_{3/2}$ on the calcium concentration in $La_{1-x}Ca_xMnO_{3\pm\delta}$; (d) the dependence of the exchange splitting energy for the Mn3s level (ΔS) in $La_{1-x}Ca_xMnO_{3+\delta}$ on the number of electrons in the d shell of manganese (n); (1) $LaMnO_3$, (2) $La_{0.94}Ca_{0.06}MnO_3$, (3) $La_{0.90}Ca_{0.1}MnO_3$, (4) $La_{0.80}Ca_{0.20}MnO_3$, (5) $La_{0.70}Ca_{0.30}MnO_3$, (6) $La_{0.50}Ca_{0.50}MnO_3$, (7) $CaMnO_3$, (8) $LaMnO_{2.98}$, (9) $LaMnO_{3.15}$, (10) $La_{0.90}Ca_{0.10}MnO_{3.09}$, (11) $La_{0.80}Ca_{0.20}MnO_{3.02}$; (○) corresponds to a *Pnma* structure, (•) to a $P112_1/c$ structure, and (■) to a $R\bar{3}c$ structure.

shell (which decreases as the oxidation state of the manganese rises) [3, 4, 14]. As with the preceding method for determining the valence, the "charging" of the samples has no effect on the accuracy of the measurements. One disadvantage of this method as applied to lanthanum might be the substantial overlap of the Mn3s spectrum by an x-ray satellite of the La4$d_{5/2}$ peak (for both aluminum and magnesium anodes in the x-ray source).

The inset to Fig. 3b shows a spectrum of Mn3s for $La_{0.7}Ca_{0.3}MnO_3$, which is typical of the other compositions as well. The absence of an x-ray satellite of the La4$d_{5/2}$ peak is explained by the fact that in the course of the mathematical processing it was subtracted from the overall spectrum. The found values of ΔS, as well as the positions of the low energy peak (see Fig. 3b) have a quite distinct dependence on the calcium concentration and, therefore, on the oxidation state of the manganese.

Table 3 lists the binding energies of Mn3s (the low energy peak) and the values of the exchange splitting for samples with and without excess oxygen. It should be pointed out at once that the exchange splitting of Mn3s for low values of x gives a much better identification of the state of the manganese ion in solid solution than does the binding energy. It is quite evident that ΔS for the oxidized samples ($\delta > 0$) is considerably lower than for the unoxidized samples ($\delta = 0$); this should [3, 4] correspond to a higher average valence for the manganese ions. The data of Table 3 show that a similar magnitude of the shift ΔS (and corresponding change in the concentration of Mn^{4+}) can be obtained by an alternative method (cation substitution, x), but this takes place at twice (relative to δ) the doping level. This result is in good agreement with the physical and chemical principles of charge compensation, which can be written formally for $La_{1-x}Ca_xMnO_{3+\delta}$ as follows:

TABLE 3. Binding Energy and Exchange Splitting of the X-Ray Photoelectron Peak Mn3*s* in $La_{1-x}Ca_xMnO_{3+\delta}$ Solid Solution

Composition	E_b, eV	ΔS, eV
$LaMnO_3$	83.02	6.90
$LaMnO_{3.15}$	83.11	6.25
$La_{0.9}Ca_{0.1}MnO_3$	83.10	6.58
$La_{0.90}Ca_{0.10}MnO_3$	83.12	6.43
$La_{0.8}Ca_{0.2}MnO_3$	83.11	6.34
$La_{0.80}Ca_{0.20}MnO_{3.02}$	83.13	6.30
$La_{0.7}Ca_{0.3}MnO_3$	83.25	5.91
$La_{0.5}Ca_{0.5}MnO_3$	83.43	5.83
$CaMnO_3$	83.57	4.75

$$La(Mn^{3+})O_3 + \delta/2O_2 \leftrightarrow La(Mn^{3+})_{1-2\delta}(Mn^{4+})_{2\delta}O_{3+\delta}\,, \quad (1)$$

$$(1-x)La(Mn^{3+})O_3 + xCa(Mn^{4+})O_3 \leftrightarrow La_{1-x}Ca_x(Mn^{3+})_{1-x}(Mn^{4+})_xO_{3+\delta}\,. \quad (2)$$

According to Fig. 3, the presence of Mn^{2+} ions in a $La_{1-x}Ca_xMnO_{3+\delta}$ solid solution is improbable. Furthermore, an attempt to confirm this by means of a proper study of exchange splitting for reduced $LaMnO_3$ containing a substantial amount of Mn^{2+} ions was unsuccessful because of almost complete overlap of the x-ray satellite of La4*d* with the spectrum of Mn3*s* that was being studied.

Therefore, the exchange splitting of Mn3s we have measured in samples of $La_{1-x}Ca_xMnO_{3+\delta}$, $\delta > 0$ with Mn3*s* (see Table 3) indicates that the state of the manganese ions in the oxidized solid solution corresponds to an intermediate state between Mn^{3+} and Mn^{4+}. Compared to analogous compositions with respect to calcium, but without excess oxygen, the Mn^{4+} component is more pronounced in this mixed state. These results are consistent with [15], where the valence of the manganese was estimated by another alternative means, studying the intensity and position of the Mn2$p_{1/2}$ satellite.

The difficulties in identifying the coexisting states of manganese and in interpreting the corresponding spectra are still related to the fact that its reflections are, by nature, broad and nonsymmetric. This shows up, in particular, in the attempts by several authors to carry out a detailed analysis of the intense Mn2$p_{3/2}$ peak by separating the signals from different states of manganese (e.g., [16]). A more informative method for determining the proportion $Mn^{2+}/Mn^{3+}/Mn^{4+}$ may be to account for the asymmetry in the peaks, which is a consequence of the "shakeout" effect for the metals [17, 18]. However, in a study of the solid solution $La_{1-x}Me_xMnO_{3+\delta}$ for small *x*, these methods did not yield satisfactory results. In addition, an analysis of the corresponding spectrum for samples with different calcium contents showed that the type of crystalline structure of the $La_{1-x}Ca_xMnO_{3+\delta}$ has a significant effect on the binding energy for the Mn2$p_{3/2}$ spectrum line (Fig. 3c).

Our x-ray structure analyses of the solid solution $La_{1-x}Ca_xMnO_{3+\delta}$ show that compositions with x = 0.1–0.3 have an orthorhombic (O) crystal system with unit cell parameters $a < \sqrt{2}b < c$. As the degree of calcium doping is increased, the unit cell approaches pseudocubic (C). In the monoclinic structure of $LaMnO_3$ and $La_{0.94}Ca_{0.06}MnO_3$ samples that are stoichiometric with respect to oxygen the proportions of the unit cell parameters are different: $a > c > \sqrt{2}b$. The difference in the lattice metric for the polymorphic modifications of lanthanum manganite is caused by a change in the average ionic radii in the A- and B-positions of the perovskite-like structure (ABO3). In addition, the resulting slope and rotation of the MnO_6 octahedrons enhance the nonequivalence of the Mn–O bond lengths. When there is a large oxygen excess, the samples crystallize in a rhombohedral (R) system with equal Mn–O bonds in the manganese-oxygen octahedra.

In light of the x-ray structural data obtained here, the dependences of the binding energy of the Mn2$p_{3/2}$ peak on the composition parameter *x* (Fig. 3c) show that immediately upon the transition from a monoclinic structure

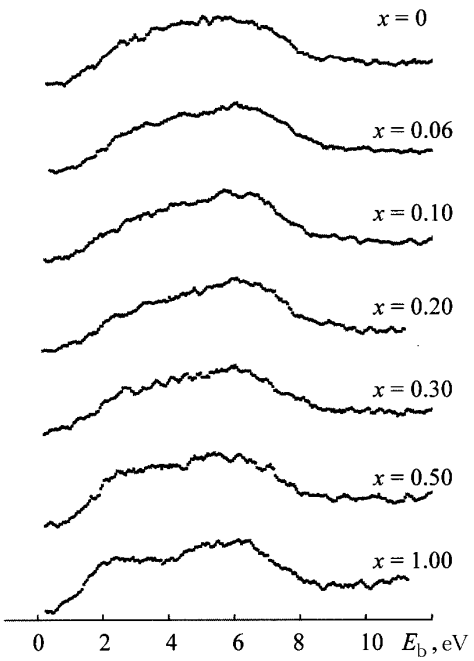

Fig. 4. Normalized spectra of the valence band of $La_{1-x}Ca_xMnO_{3+\delta}$

(x = 0.00, 0.06) to an orthorhombic structure (x > 0.06), the binding energy changes discontinously, and then increases monotonically as x rises to 0.50. Given this, we may assume that it is not so much the effective charge concentrated on the manganese ions that affects the position of the Mn2$p_{3/2}$ peak, as the Madelung energy which characterizes the effect of the crystal field on the average with respect to the oxide. This is substantially reinforced by data on E_b (for Mn2$p_{3/2}$) for a sample synthesized with a low partial pressure of oxygen which, therefore, had a high oxygen deficit ($O_{2.89}$) and corresponding number of Mn^{2+} ions. (See Fig. 3c.) Despite the presence of an excess negative charge on the manganese ions, the binding energy of Mn2$p_{3/2}$ for this sample remained at the level of E_b for the other samples that were isotructural to it.

Spectrum of the valence band. Computational studies of the valence band of different $La_{1-x}Ca_xMnO_{3+\delta}$ compositions [19] have shown that the major contribution to the spectrum of the valence band is from the O2p states of oxygen (at ~6 eV) and the Mn3d states of manganese (at 3.5 eV), while the contributions of the valence electrons of lanthanum and calcium are relatively small. A study has been made [4] of the valence band of the manganites, with a simultaneous examination of the exchange splitting of the Mn3s electronic level. The exchange splitting was found to depend on the formal charge on the manganese and a relationship was found between the valence band of the manganites and the spectrum of Mn3s on comparison with the data of [10]. According to the experimental data from [4], no significant changes in the magnitude of the exchange splitting of Mn3s was observed for doped manganites with formal charge states for the Mn ranging from 3+ to 3.3+. This implies that the electron holes arising in the structure of the manganites at these doping levels lie near oxygen atoms.

Figure 4 shows some of our experimental spectra of $La_{1-x}Ca_xMnO_{3+\delta}$ in which two peaks can be seen, at 3.5 and 6.0 eV. These correspond to signals from the Mn3d and O2p electronic levels, respectively [19]. The intensity ratio of these peaks changes significantly when La is replaced by Ca. The increase in the intensity of the Mn3d peak relative to O2p when x > 0.2 could be attributed to the migration of an electron hole from the d orbital of Mn^{4+} to the p orbital of O^{2-} implied by the results of [4]. At the same time, unlike in [4], we obtained an entirely opposite result for the exchange splitting of the Mn3s level within this range of x. (See Table 3.) In our case, it changes significantly, thereby indicating localization of the electron holes right on the manganese. Thus, we have tried to explain the observed variations in the spectrum of the valence band in a different way: by adding a Ca3s signal, which increases as the concentration of calcium in the oxide is raised, to the Mn3d peak.

Conclusion. The reduction in the exchange splitting of Mn3*s* and the increasing difference between the binding energies of Mn2$p_{3/2}$ and O1*s* as the concentration of calcium in $La_{1-x}Ca_xMnO_{3+\delta}$ solid solutions is raised show that in all the compositions studied here there is a high probability that Mn^{3+} and Mn^{4+} ions coexist, while Mn^{2+} is unlikely to be present. All the electron holes formed by doping lanthanum manganite will be localized at manganese ions (there is no singly valent oxygen in the oxide). In addition, the observed significant shifts in the Ca*p*, La3*d*, and O1*s* lines toward lower binding energies, as well as the (slight) simultaneous opposite shift of Mn2*p*, as the concentration parameter *x* is increased were all unexpected. They cannot be explained just by charge redistribution over the directions of the anion-cation bonds. On the other hand, the substantial effect of the crystalline structure of the solid solution on the spectrum of manganese (and, to some extent, on the spectra of the other elements) is indicative of the large role played by the crystalline field (the Madelung energy) in the oxide. Getting a more exact understanding of the role of the crystalline field in the behavior of the Ca2*p*, La3*d*, and O1*s* spectra that we have observed will require additional experimental and theoretical study.

Acknowledgments. We thank Dr. M. V. Kuznetsov (Institute of Solid State Chemistry, Urals Branch of the Russian Academy of Sciences) for a fruitful discussion of this paper and his comments.

This work was supported by the Russian Foundation for Basic Research (grants 07-03-00280 and 06-03-32541-a).

REFERENCES

1. J. A. M. Van Roosmalen and E. H. P. Cordfunke, *J. Solid State Chem.*, **110**, 109–112 (1994).
2. A. V. Fetisov, E. A. Pastukhov, and V. B. Fetisov, in: *Proc. Fourth Israeli-Russian bi-national Workshop*, June 19–25, 2005, Jerusalem-Tel Aviv (2005), pp. 76–84.
3. T. Saitoh, A. E. Bocquet, T. Mizokawa, A. Fujimori, M. Abbate, Y. Takeda, and M. Takano, *Phys. Rev. B*, **51**, 13942–13951 (1995).
4. V. R. Galakhov, M. Demeter, S. Bartkowski, M. Neumann, N. A. Ovechkina, E. Z. Kurmaev, N. I. Lobachevskaya, Ya. M. Mukovskii, J. Mitchell, and D. L. Ederer, *Phys. Rev. B*, **65**, 113102 (2002).
5. T. A. Tyson, Q. Qian, C.-C. Kao, J.-P. Rueff, F. M. F. de Groot, M. Croft, S.-W. Cheong, M. Greenblatt, and M. A. Subramanian, *Phys. Rev. B*, **60**, 4665–4674 (1999).
6. P. Decorse, G. Caboche, and L.-C. Dufour, *Solid State Ionics*, **117**, 161–169 (1999).
7. V. F. Balakirev, S. H. Estemirova, A. M. Yankin, and S. G. Titova, *Dokl. RAN*, **416**, No. 2, 206–208 (2007).
8. S. Mathur and H. Shen, *J. Sol-Gel Sci. Technol.*, **25**, 147–157 (2002).
9. E. Talika, A. Novosselov, M. Kulpa, and A. Pajaczkowska, *J. Alloys and Compounds*, **321**, 24–26 (2001).
10. R. W. M. Kwok, XPS Peak Fitting Program for WIN95/98 XPSPEAK Version 4.1. (2000), http://www.phy.cuhk.edu.hk/~surface/XPSPEAK/
11. A. N. Chaika, A. M. Ionov, N. A. Tulina, D. A. Shulyatev, and Ya. M. Mukovskii, *J. Electron Spectrosc. and Relat. Phenomena*, **148**, 101–106 (2005).
12. M. F. Hundley and J. J. Neumaier, *Phys. Rev. B*, **55**, 11511 (1997).
13. V. Di Castro and G. Polzonetti, *J. Electron Spectrosc. Relat. Phenomena*, **48**, 117–123 (1989).
14. A. Kowalczyk, A. Slebarski, A. Szajek, J. Baszynski, and A. Winiarski, *J. Magnetism and Magnet. Mater.*, **212**, 107–111 (2000).
15. M. Abbate, F. Prado, and A. Caneiro, *Solid State Commun.*, **123**, 81–85 (2002).
16. Q. Zhou, M. Dai, R. Wang, L. Jin, S. Zhu, L. Qian, Y. Wu, and J. Feng, *Physica B*, **391**, 206–211 (2007).
17. J. W. Liu, G. Chen, Z. H. Li, W. W. An, and Z. G. Zhang, *J. Alloys and Compounds*, **431**, 1–5 (2007).
18. S. P. Kowalczyk, L. Ley, F. R. McFeely, and D. A. Shirley, *Phys. Rev. B*, **11**, 1721–1727 (1975).
19. R. Zalecki, A. Kolodziejczyk, Cz. Kapusta, and K. Krop, *J. Alloys and Compounds*, **328**, 175–180 (2001).